# On the use of the Linear Sampling Method to identify cracks in elastic waveguides

**L. Bourgeois, E. Lunéville**

Laboratoire POEMS, UMR ENSTA/CNRS/INRIA, Ecole Nationale Supérieure des Techniques Avancées, 828, Boulevard des Maréchaux, 91762 Palaiseau Cedex, France

**Abstract.** We consider the identification of cracks in an elastic 2D or 3D waveguide with the help of a modal version of the Linear Sampling Method. The main objective of our paper is to show that since the usual crack in elasticity is traction free, that is the boundary condition on the lips of the crack is *a priori* known to be of Neumann type, we shall adapt the formulation of the sampling method to such boundary condition in order to improve the efficiency of the method. The need for such adaptation is proved theoretically and illustrated numerically with the help of 2D examples.

## 1. Introduction

The identification of unknown cracks in an elastic waveguide by measuring the scattered waves which result from the interaction between several known incident waves and such cracks is a problem of practical interest. It arises for example in the ultrasonic Non Destructive Testing (NDT) of tubular metallic structures. In this paper we use the Linear Sampling Method (LSM) introduced in [14] and generalized in [9] in order to solve such inverse scattering problem in the frequency domain. The Linear Sampling Method belongs to the wide class of the so-called "qualitative methods" or "sampling methods", which are described in [18] and which consist in checking, for any point of a sampling domain, if such point belongs to the defect or not by solving a small system depending only on the data. There are many contributions dealing with qualitative methods in elasticity for penetrable or impenetrable obstacles with non empty interior, for instance [2, 10, 21, 11, 13]. But to our best knowledge, our paper is the first attempt to apply a qualitative method to detect cracks in elasticity.

In fact we have to face at least two difficulties. The first one is the fact that by definition the crack is an obstacle with empty interior. In such case, the justification of the sampling methods is specific, as exposed in [19, 9, 5] in the acoustic case. The second one concerns the geometry of the background medium, which is bounded in all directions of space but one. In such case, the identification of defects is more difficult than in free space, because

the scattered field contains an evanescent part that decays exponentially far away from the defect, as detailed in [7]. The application of sampling methods to an acoustic waveguide bounded in all directions but one is already addressed in [24, 12, 7], while the case of the elastic waveguide is analyzed in [6].

In the restricted case of acoustics, these two difficulties were addressed at the same time in a first contribution of the authors [8], which in particular insists on the fact that whenever the boundary condition on the crack is *a priori* known (for example of Dirichlet or Neumann type) then the test function used in the formulation of the sampling method has to be properly chosen in order to improve the quality of the identification. In the case of the Neumann boundary condition, this choice also implies an optimization procedure to identify the unit normal vector to the crack, following an idea introduced in [5]. An important specificity of [8] is the fact that we used a modal formulation of the Linear Sampling Method and of the Factorization Method of A. Kirsch [18], which is specific to the waveguide geometry and was first introduced in [7]. In such formulation, the incident waves do not consist of point sources like in a classical near field formulation but consist of guided modes. The main advantage of the modal formulation is that it enables us to introduce a far field formulation, which is natural when the measurements take place far away from the cracks, as it is frequent in NDT applications.

From the point of view of applications, the case of elasticity is more interesting than the case of acoustics because of ultrasonic NDT, in particular the most common defects we expect in a metallic structure are traction free cracks (that is a boundary condition of Neumann type is prescribed on the lips of the crack). This is why we tackle the case of elasticity in the present paper, and our contribution in [8] in the case of acoustics can be considered as a first step to address this more challenging case. It happens that in elasticity, the displacement field can no more be projected on a transverse basis as it is done in acoustics (see [8]), which is due to the "bad" spectral properties of the elasticity operator. A way to cope with this situation, as detailed in [3], is to introduce some special vector variables that mix the components of displacement and the components of the column of the stress tensor which is associated with the direction of propagation. The modal formulation of the LSM with the help of such mixed variables to identify Dirichlet obstacles was already presented in [6]. We use the same mixed variables in the present paper in the case of cracks. Note that our results in the elastic case rely on two usual conjectures: one concerns the completeness of the transverse modes in terms of our mixed vector variables, the other one concerns well posedness of the forward problem.

Our paper is organized as follows. In section 2 we present the forward and inverse problems for cracks in elasticity, and we recall in particular the main results of [3]. The Linear Sampling Method is then introduced in section 3, in particular in the modal form. We complete this section by some numerical experiments in 2D.

## 2. The forward and inverse problems

### *2.1. The formalism of mixed variables*

The waveguide we consider is the domain $W = S \times \mathbb{R}$ in $\mathbb{R}^d$ with $d = 2$ or $d = 3$. The following analysis is valuable both in 2D and in 3D. In 2D, $S$ denotes the interval $(-h, h)$, where $h > 0$, while in 3D, $S$ denotes a bounded and open domain of $\mathbb{R}^2$, the boundary of which is smooth and denoted by $\Gamma$. A generic point $x$ of $W$ has coordinates $x = (x_S, x_3)$, where $x_S \in S$ is the coordinate in the transverse section and $x_3 \in \mathbb{R}$ is the coordinate in the direction of propagation.

The behaviour of the material is characterized by linear isotropic elasticity: the Lamé coefficients are denoted by $\lambda, \mu$ with $\lambda + 2\mu > 0$ and $\mu > 0$, while the density is denoted by $\rho > 0$. In the elastic waveguide, for a given fixed frequency $\omega$, we first consider the displacement fields $\mathbf{u}$ given by the system

$$\left\{ \begin{array}{rcl} \mathrm{div}\sigma(\mathbf{u}) + \rho\omega^2\mathbf{u} = 0 & \text{in} & W \\ \sigma(\mathbf{u}) \cdot \boldsymbol{\nu} = 0 & \text{on} & \Gamma. \end{array} \right. \tag{1}$$

In the system (1) above, $\boldsymbol{\nu}$ denotes the outward unit normal and the stress tensor $\sigma$ is given by

$$\sigma(\mathbf{u}) = \lambda \mathrm{div}(\mathbf{u})\,\mathrm{Id} + 2\mu\,\varepsilon(\mathbf{u}) \quad \text{with} \quad \varepsilon(\mathbf{u}) = \frac{1}{2}\left(\nabla\mathbf{u} + {}^T\nabla\mathbf{u}\right),$$

where Id denotes the identity matrix, ${}^T\cdot$ is the transposed of a tensor and $\varepsilon(\mathbf{u})$ denotes the strain tensor.

Solving the system (1) is a much more complicated task as in the acoustic case, since in elasticity we are not able to find a complete basis in the transverse section $S$ only in terms of the displacement, that is the analogous of the $\theta_n$ introduced in [8]. We hence introduce the formalism of [3] in the 3D case exactly as in [6]. It consists in defining some new vector variables $\mathbf{X}$ and $\mathbf{Y}$ that mix the components of the displacement $\mathbf{u}$ and the components of the vector $\sigma \cdot \boldsymbol{e}_3$, where $\boldsymbol{e}_3$ is the unit vector following the direction of propagation $x_3$. We introduce such notations in the 3D case, but they are also consistent in the 2D case provided the subscript 2 disappears in the equations.

Precisely, from the vectors $\mathbf{u} = (\mathbf{u}_S, \mathsf{u}_3)$ and $\sigma(\mathbf{u}) \cdot e_3 = (\mathbf{t}_S, -\mathsf{t}_3)$, the mixed variables are defined by

$$\mathbf{X} = \begin{pmatrix} \mathbf{t}_S \\ \mathsf{u}_3 \end{pmatrix} \quad \text{and} \quad \mathbf{Y} = \begin{pmatrix} \mathbf{u}_S \\ \mathsf{t}_3 \end{pmatrix}.$$

The mixed variables $\mathbf{X}$ and $\mathbf{Y}$ were introduced in [16] and revisited in [22]. Clearly, $\mathbf{X}$ and $\mathbf{Y}$ are uniquely calculated from the displacement field $\mathbf{u}$, and will be sometimes hereafter called the $\mathbf{X}$ and $\mathbf{Y}$ extensions of $\mathbf{u}$.

**Remark 2.1.** *The mixed variables* $\mathbf{X}$ *and* $\mathbf{Y}$ *naturally appear when one wants to apply the method of images to elasticity. Indeed, a symmetric displacement field* $\mathbf{u}$ *with respect to the plane* $\{x_3 = 0\}$ *does not satisfy* $\sigma \cdot \boldsymbol{e}_3 = 0$ *on that plane but satisfies* $\mathbf{Y} = 0$*. Similarly, an antisymmetric displacement field* $\mathbf{u}$ *with respect to the plane* $\{x_3 = 0\}$ *does not satisfy* $\mathbf{u} = 0$ *on that plane but satisfies* $\mathbf{X} = 0$*. This is a new situation compared to the acoustic case.*

By an easy calculation (see [3]), it can be proved that the system (1) is equivalent to the "evolution" problem:

$$\frac{\partial}{\partial x_3}\begin{pmatrix} \mathbf{X} \\ \mathbf{Y} \end{pmatrix} = \begin{pmatrix} 0 & F_Y \\ F_X & 0 \end{pmatrix}\begin{pmatrix} \mathbf{X} \\ \mathbf{Y} \end{pmatrix}, \tag{2}$$

where

$$F_Y\mathbf{Y} = \begin{pmatrix} -\mathrm{div}\sigma_S(\mathbf{Y}) - \rho\omega^2\mathbf{u}_S \\ -\alpha \mathrm{div}_S\mathbf{u}_S - \dfrac{\alpha}{\lambda}\mathsf{t}_3 \end{pmatrix} \quad \text{and} \quad F_X\mathbf{X} = \begin{pmatrix} \dfrac{\mathbf{t}_S}{\mu} - \nabla_S\mathsf{u}_3 \\ \mathrm{div}_S\mathbf{t}_S + \rho\omega^2\mathsf{u}_3 \end{pmatrix},$$

and the boundary conditions on $\Gamma$:

$$\begin{cases} \sigma_S(\mathbf{Y}) \cdot \boldsymbol{\nu}_S = 0, \\ \mathbf{t}_S \cdot \boldsymbol{\nu}_S = 0. \end{cases} \tag{3}$$

Here we have used the notations

$$\sigma_S = \begin{pmatrix} \sigma_{11} & \sigma_{12} \\ \sigma_{21} & \sigma_{22} \end{pmatrix}, \quad \varepsilon_S = \begin{pmatrix} \varepsilon_{11} & \varepsilon_{12} \\ \varepsilon_{21} & \varepsilon_{22} \end{pmatrix}, \quad \boldsymbol{\nu}_S = (\nu_1, \nu_2),$$

$$\mathrm{div}_S\mathbf{u}_S = \frac{\partial u_1}{\partial x_1} + \frac{\partial u_2}{\partial x_2}, \quad \nabla_S\phi = \frac{\partial \phi}{\partial x_1}\,\boldsymbol{e}_1 + \frac{\partial \phi}{\partial x_2}\,\boldsymbol{e}_2,$$

$$\delta = \frac{2\lambda\mu}{\lambda + 2\mu}, \quad \alpha = \frac{\lambda}{\lambda + 2\mu}.$$

Lastly, the expression of $\sigma_S(\mathbf{Y})$ is

$$\sigma_S(\mathbf{Y}) = (\delta \mathrm{div}_S\mathbf{u}_S - \alpha\mathsf{t}_3)\mathrm{Id} + 2\mu\varepsilon_S(\mathbf{u}_S).$$

Our further developments rely on the fact, which is proved in [3], that except for a countable set of frequencies $\omega$, the solutions of problem (2) (3) are of the form

$$\begin{pmatrix} \mathbf{X} \\ \mathbf{Y} \end{pmatrix} = \sum_{n>0} a_n^+ \begin{pmatrix} \mathbf{X}_n^+ \\ \mathbf{Y}_n^+ \end{pmatrix} + a_n^- \begin{pmatrix} \mathbf{X}_n^- \\ \mathbf{Y}_n^- \end{pmatrix} \tag{4}$$

with

$$\begin{pmatrix} \mathbf{X}_n^\pm(x) \\ \mathbf{Y}_n^\pm(x) \end{pmatrix} = \begin{pmatrix} \pm\boldsymbol{\mathcal{X}}_n(x_S) \\ \boldsymbol{\mathcal{Y}}_n(x_S) \end{pmatrix} e^{\pm i\beta_n x_3}, \tag{5}$$

where the eigenmodes $(\beta_n, \boldsymbol{\mathcal{X}}_n, \boldsymbol{\mathcal{Y}}_n)_{n>0}$ are obtained by searching the rightgoing solutions $(\mathbf{X}, \mathbf{Y})$ of problem (2) (3) of the particular form

$$\begin{pmatrix} \mathbf{X} \\ \mathbf{Y} \end{pmatrix} = \begin{pmatrix} \boldsymbol{\mathcal{X}}(x_S) \\ \boldsymbol{\mathcal{Y}}(x_S) \end{pmatrix} e^{i\beta x_3}.$$

An essential result (see [3]) concerning theses eigenmodes is the following biorthogonality relationship:

$$(\boldsymbol{\mathcal{X}}_n | \boldsymbol{\mathcal{Y}}_m)_S = \delta_{nm} J_n$$

for some constant $J_n$, and the bilinear form $(\cdot|\cdot)_S$ is defined for $\boldsymbol{\mathcal{X}}, \boldsymbol{\mathcal{Y}} \in \mathbf{L}^2(S) := (L^2(S))^3$ by

$$(\boldsymbol{\mathcal{X}}|\boldsymbol{\mathcal{Y}})_S = \int_S (\mathcal{X}_1\mathcal{Y}_1 + \mathcal{X}_2\mathcal{Y}_2 + \mathcal{X}_3\mathcal{Y}_3)\, ds = \int_S (\boldsymbol{u}_S \cdot \boldsymbol{t}_S + t_3 u_3)\, ds, \tag{6}$$

and extended to the case when $\boldsymbol{\mathcal{X}} \in (\tilde{H}^{-\frac{1}{2}}(S))^2 \times H^{\frac{1}{2}}(S)$ and $\boldsymbol{\mathcal{Y}} \in (H^{\frac{1}{2}}(S))^2 \times \tilde{H}^{-\frac{1}{2}}(S)$, where $\tilde{H}^{-\frac{1}{2}}(S)$ is the dual space of $H^{\frac{1}{2}}(S)$.
With assumption

**Assumption 2.2.** *$\omega$ is such that $\beta_n \neq 0$ and $J_n \neq 0$ for all $n > 0$.*

then the eigenmodes $(\beta_n, \boldsymbol{\mathcal{X}}_n, \boldsymbol{\mathcal{Y}}_n)$ can be organized in two families:

- the rightgoing modes $(\beta_n, \boldsymbol{\mathcal{X}}_n, \boldsymbol{\mathcal{Y}}_n)_{n>0}$, which correspond to $\mathrm{Im}(\beta_n) > 0$ (for non-propagating modes) or $\frac{\partial\omega}{\partial\beta_n} > 0$ (for propagating modes),
- the leftgoing modes $(\beta_{-n}, \boldsymbol{\mathcal{X}}_{-n}, \boldsymbol{\mathcal{Y}}_{-n})_{n>0} = (-\beta_n, -\boldsymbol{\mathcal{X}}_n, \boldsymbol{\mathcal{Y}}_n)_{n>0}$.

The non-propagating modes can themselves be split into evanescent modes ($\beta_n$ is purely imaginary) and inhomogeneous modes ($\beta_n$ is not purely imaginary).
It results from this $(\mathbf{X}, \mathbf{Y})$-analysis that with the notations

$$\boldsymbol{\mathcal{X}}_n = \begin{pmatrix} \boldsymbol{t}_S^n \\ u_3^n \end{pmatrix} = \begin{pmatrix} t_1^n \\ t_2^n \\ u_3^n \end{pmatrix} \quad \text{and} \quad \boldsymbol{\mathcal{Y}}_n = \begin{pmatrix} \boldsymbol{u}_S^n \\ t_3^n \end{pmatrix} = \begin{pmatrix} u_1^n \\ u_2^n \\ t_3^n \end{pmatrix}, \tag{7}$$

the solutions of problem (1) are combinations of the guided modes

$$\mathbf{U}_n^{\pm}(x) = \begin{pmatrix} \boldsymbol{u}_S^n(x_S) \\ \pm u_3^n(x_S) \end{pmatrix} e^{\pm i\beta_n x_3}. \tag{8}$$

In the following, thank's to assumption 2.2 we can normalize the $\boldsymbol{\mathcal{X}}_n$ and the $\boldsymbol{\mathcal{Y}}_n$ (without change in their notations) in such a way that $(\boldsymbol{\mathcal{X}}_n|\boldsymbol{\mathcal{Y}}_m)_S = \delta_{nm}$. We now introduce a first conjecture, that is completeness of the eigenmodes, which seems an open question to the authors' knowledge.

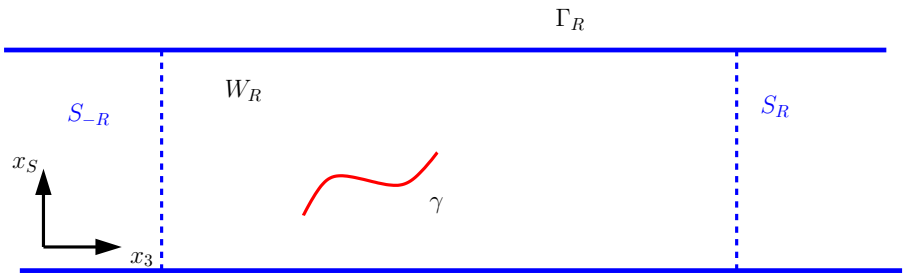


**Figure 1.** Geometry of the waveguide

**Conjecture 2.3.** *For every* $\boldsymbol{\mathcal{X}} = (\boldsymbol{t}_S, u_3) \in (\tilde{H}^{-\frac{1}{2}}(S))^2 \times H^{\frac{1}{2}}(S)$ *we have*

$$\boldsymbol{\mathcal{X}} = \sum_{n>0} (\boldsymbol{\mathcal{X}}|\boldsymbol{\mathcal{Y}}_n)_S \boldsymbol{\mathcal{X}}_n, \tag{9}$$

*for every* $\boldsymbol{\mathcal{Y}} = (\boldsymbol{u}_S, t_3) \in (H^{\frac{1}{2}}(S))^2 \times \tilde{H}^{-\frac{1}{2}}(S)$ *we have*

$$\boldsymbol{\mathcal{Y}} = \sum_{n>0} (\boldsymbol{\mathcal{X}}_n|\boldsymbol{\mathcal{Y}})_S \boldsymbol{\mathcal{Y}}_n, \tag{10}$$

*and there exist* $c, C > 0$ *such that*

$$c\,||\boldsymbol{\mathcal{X}}||^2_{(\tilde{H}^{-\frac{1}{2}}(S))^2 \times H^{\frac{1}{2}}(S)} \leq \sum_{n>0} |(\boldsymbol{\mathcal{X}}|\boldsymbol{\mathcal{Y}}_n)_S|^2 \leq C\,||\boldsymbol{\mathcal{X}}||^2_{(\tilde{H}^{-\frac{1}{2}}(S))^2 \times H^{\frac{1}{2}}(S)}$$

$$c\,||\boldsymbol{\mathcal{Y}}||^2_{(H^{\frac{1}{2}}(S))^2 \times \tilde{H}^{-\frac{1}{2}}(S)} \leq \sum_{n>0} |(\boldsymbol{\mathcal{X}}_n|\boldsymbol{\mathcal{Y}})_S|^2 \leq C\,||\boldsymbol{\mathcal{Y}}||^2_{(H^{\frac{1}{2}}(S))^2 \times \tilde{H}^{-\frac{1}{2}}(S)}.$$

*Decompositions (9) and (10) are also true for* $\boldsymbol{\mathcal{X}} \in \mathbf{L}^2(S)$ *and* $\boldsymbol{\mathcal{Y}} \in \mathbf{L}^2(S)$.

### *2.2. Statement of the problems*

Following [9], a crack $\gamma$ is defined as a portion of a smooth nonintersecting curve ($d = 2$) or surface ($d = 3$) that encloses a domain $D$ in $W$, such that for $d = 3$ its boundary $\partial\gamma$ is smooth, and $\overline{\gamma} \in W$. We assume that $\gamma$ is an open set with respect to the induced topology on $\partial D$. The normal vector $\boldsymbol{\nu}$ on $\gamma$ is defined as the outward normal vector to $D$. If we denote $S_s = S \times \{s\}$ any transverse section, we assume that $\overline{\gamma}$ lies between sections $S_{-R}$ and $S_R$ for some $R > 0$. Then $W_R$ and $\Gamma_R$ denote the portions of $W$ and $\Gamma$ which are limited by $S_{-R}$ and $S_R$ (see figure 1).

In order to introduce the forward problem we consider, we need to define some spaces and some surface operators on $S_{\pm R}$ in order to restrict our problem to the bounded domain $W_R$. We denote by $H^{\frac{1}{2}}(\gamma)$ the set of all restrictions to $\gamma$ of functions in $H^{\frac{1}{2}}(\partial D)$, $\tilde{H}^{\frac{1}{2}}(\gamma)$ the subspace of $H^{\frac{1}{2}}(\gamma)$ which consists of functions on $\gamma$ such that their extension by 0 on $\partial D$ belong to $H^{\frac{1}{2}}(\partial D)$. In addition we consider $H^{-\frac{1}{2}}(\gamma)$ and $\tilde{H}^{-\frac{1}{2}}(\gamma)$ the dual spaces of $\tilde{H}^{\frac{1}{2}}(\gamma)$ and $H^{\frac{1}{2}}(\gamma)$, respectively (see for example [9]). Note that the space $H^{-\frac{1}{2}}(\gamma)$ can be identified

as the set of all restrictions to $\gamma$ of distributions in $H^{-\frac{1}{2}}(\partial D)$, while $\tilde{H}^{-\frac{1}{2}}(\gamma)$ can be identified as the set of all distributions of $H^{-\frac{1}{2}}(\partial D)$ the support of which is contained in $\overline{\gamma}$. Lastly, we define $\mathbf{H}^{\frac{1}{2}}(\gamma) := (H^{\frac{1}{2}}(\gamma))^3$ as well as $\tilde{\mathbf{H}}^{\frac{1}{2}}(\gamma)$, $\mathbf{H}^{-\frac{1}{2}}(\gamma)$ and $\tilde{\mathbf{H}}^{-\frac{1}{2}}(\gamma)$.
Following [3], the eigenmodes $(\beta_n, \boldsymbol{\mathcal{X}}_n, \boldsymbol{\mathcal{Y}}_n)_{n>0}$ and the conjecture 2.3 enable us to define a continuous $\boldsymbol{\mathcal{Y}}$-to-$\boldsymbol{\mathcal{X}}$ operator $T_\pm$ acting on transverse sections $S_{\pm R}$, precisely $T_\pm : (H^{\frac{1}{2}}(S_{\pm R}))^2 \times \tilde{H}^{-\frac{1}{2}}(S_{\pm R}) \to (\tilde{H}^{-\frac{1}{2}}(S_{\pm R}))^2 \times H^{\frac{1}{2}}(S_{\pm R})$, such that

$$T_\pm \boldsymbol{\mathcal{Y}} = \sum_{n>0} (\boldsymbol{\mathcal{X}}_n | \boldsymbol{\mathcal{Y}})_{S_{\pm R}} \boldsymbol{\mathcal{X}}_n.$$

We are now in a position to introduce the forward Dirichlet/Neumann crack problem.
For $\boldsymbol{f} \in \mathbf{H}^{\frac{1}{2}}(\gamma)$ and $\boldsymbol{g} \in \mathbf{H}^{-\frac{1}{2}}(\gamma)$ we consider the scattering problem: find $\mathbf{u} \in \mathbf{H}^1(W_R \setminus \gamma) := (H^1(W_R \setminus \gamma))^3$ such that

$$\left\{ \begin{array}{ccc} \mathrm{div}\sigma(\mathbf{u}) + \rho\omega^2 \mathbf{u} = 0 & \text{in} & W_R \setminus \overline{\gamma} \\ \sigma(\mathbf{u}) \cdot \boldsymbol{\nu} = 0 & \text{on} & \Gamma_R \\ \mathbf{u}_\pm = \boldsymbol{f} \quad \text{or} \quad \sigma(\mathbf{u}_\pm) \cdot \boldsymbol{\nu} = \boldsymbol{g} & \text{on} & \gamma \\ T_\pm \mathbf{Y} = \pm \mathbf{X} & \text{on} & S_{\pm R}, \end{array} \right. \tag{11}$$

where $\mathbf{u}_\pm$ and $\sigma(\mathbf{u}_\pm) \cdot \boldsymbol{\nu}$ denote the trace of the displacement and the trace of the normal stress on both sides of the crack, where the sign $\pm$ is specified by the orientation of the normal $\boldsymbol{\nu}$ on $\gamma$. The solution of problem (11) is the scattered field $\mathbf{u}^s$ associated with the incident field $\mathbf{u}^i$ with $\boldsymbol{f} = -\mathbf{u}^i|_\gamma$ or $\boldsymbol{g} = -\sigma(\mathbf{u}^i) \cdot \boldsymbol{\nu}|_\gamma$. The last equation of problem (11) is the radiation condition.
We now formulate a second conjecture:

**Conjecture 2.4.** *For $\boldsymbol{f} \in \mathbf{H}^{\frac{1}{2}}(\gamma)$ and $\boldsymbol{g} \in \mathbf{H}^{-\frac{1}{2}}(\gamma)$, the Dirichlet crack problem and the Neumann crack problem defined by (11) are well-posed in $\mathbf{H}^1(W_R \setminus \overline{\gamma})$, except for at most a countable set of $\omega$.*

**Remark 2.5.** *Such countable set of $\omega$ includes in particular those for which there exists $n > 0$ such that $\beta_n = 0$ or $J_n = 0$ (see assumption 2.2).*

In the remainder of the paper we make the following assumption:

**Assumption 2.6.** *The frequency $\omega$ is such that problem (11) is well-posed.*

**Remark 2.7.** *A weak formulation as well as a finite element formulation of problem (11) are proposed in [3]. The numerical experiments seem to provide "numerical evidence" that in general such problem is well posed, even if it is not proved yet.*

Now let us introduce the inverse problem for the elastic waveguide, with $\hat{S} := S_{-R} \cup S_R$.

**The inverse problem (IP).** *Given the measurements on $\hat{S}$ of the fields $\mathbf{X}_n^{s\pm}$, which denote the $\mathbf{X}$ extensions of the scattered fields $\mathbf{U}_n^{s\pm}$ associated with the incident fields $\mathbf{U}_n^{\pm}$ given by (8) for all $n > 0$, reconstruct the crack $\gamma$.*

## 3. The Linear Sampling Method

### *3.1. Some preliminary results*

In order to formulate the Linear Sampling Method, for convenience we use the extended outgoing Green tensor for the elastic waveguide already introduced in [6]. Such $6 \times 6$ tensor

$$G = \begin{pmatrix} G_X^X & G_X^Y \\ G_Y^X & G_Y^Y \end{pmatrix} \tag{12}$$

is such that for $y \in W$, $G(\cdot, y)$ is the solution to the following problem:

$$\left\{ \begin{array}{rcl} \dfrac{\partial}{\partial x_3} G(\cdot, y) = \begin{pmatrix} 0 & F_Y \\ F_X & 0 \end{pmatrix} G(\cdot, y) - \delta(\cdot - y) \begin{pmatrix} \mathrm{Id}_3 & 0_3 \\ 0_3 & \mathrm{Id}_3 \end{pmatrix} & \text{in} & W_R \\ \sigma_S(G(\cdot, y)) \cdot \boldsymbol{\nu}_S = 0 \quad \mathbf{t}_S(G(\cdot, y)) \cdot \boldsymbol{\nu}_S = 0 & \text{on} & \Gamma_R \\ T_\pm G_Y(\cdot, y) = \pm G_X(\cdot, y) & \text{on} & S_{\pm R}, \end{array} \right. \tag{13}$$

where $G_X$ (resp. $G_Y$) denotes the $X-$rows (resp. $Y-$rows) of matrix (12), in other words $G_X = (G_X^X \; G_X^Y)$ and $G_Y = (G_Y^X \; G_Y^Y)$. It is proved in [6] that the Green tensor $G$ is given by

$$G(x, y) = -\sum_{n>0} \begin{pmatrix} s(x_3 - y_3) \boldsymbol{\mathcal{X}}_n(x_S) \cdot {}^T \boldsymbol{\mathcal{Y}}_n(y_S) & \boldsymbol{\mathcal{X}}_n(x_S) \cdot {}^T \boldsymbol{\mathcal{X}}_n(y_S) \\ \boldsymbol{\mathcal{Y}}_n(x_S) \cdot {}^T \boldsymbol{\mathcal{Y}}_n(y_S) & s(x_3 - y_3) \boldsymbol{\mathcal{Y}}_n(x_S) \cdot {}^T \boldsymbol{\mathcal{X}}_n(y_S) \end{pmatrix} \frac{e^{i\beta_n |x_3 - y_3|}}{2}, \tag{14}$$

where $s$ is the sign function and we recall that ${}^T\cdot$ is the transposed of a tensor.
The above extended Green function is related to the classical outgoing Green tensor of the elastic waveguide $W$, denoted by $G_u^\sigma$, which is such that for $y \in W$, the $3 \times 3$ tensor $G_u^\sigma(\cdot, y)$ solves the following problem:

$$\left\{ \begin{array}{rcl} -\mathrm{div}\sigma(G_u^\sigma(\cdot, y)) - \rho\omega^2 G_u^\sigma(\cdot, y) = \delta(. - y)\mathrm{Id}_3 & \text{in} & W_R \\ \sigma(G_u^\sigma(\cdot, y)) \cdot \boldsymbol{\nu} = 0 & \text{on} & \Gamma_R \\ T_\pm G_Y^\sigma(\cdot, y) = \pm G_X^\sigma(\cdot, y) & \text{on} & S_{\pm R}, \end{array} \right. \tag{15}$$

where $G_X^\sigma$ (resp. $G_Y^\sigma$) denotes the $3 \times 3$ tensor such that each column of $G_X^\sigma$ (resp. $G_Y^\sigma$) is formed by the $\mathbf{X}$ extension (resp. $\mathbf{Y}$ extension) of the corresponding column of tensor $G_u^\sigma$.
The classical Green tensor $G_u^\sigma$ can be deduced from the extended Green tensor $G$ by selecting among the rows of matrix $G$ those who correspond to the components of $\mathbf{u}$ and by selecting among the columns of $G$ those who correspond to the components of $\sigma \cdot \boldsymbol{e}_3$.
We hence obtain by using the coordinates of $\boldsymbol{\mathcal{X}}_n$ and $\boldsymbol{\mathcal{Y}}_n$ given by (7),

$$G_u^\sigma(x, y) = -\sum_{n>0} \begin{pmatrix} u_1^n(x_S) u_1^n(y_S) & u_1^n(x_S) u_2^n(y_S) & -s(x_3 - y_3) u_1^n(x_S) u_3^n(y_S) \\ u_2^n(x_S) u_1^n(y_S) & u_2^n(x_S) u_2^n(y_S) & -s(x_3 - y_3) u_2^n(x_S) u_3^n(y_S) \\ s(x_3 - y_3) u_3^n(x_S) u_1^n(y_S) & s(x_3 - y_3) u_3^n(x_S) u_2^n(y_S) & -u_3^n(x_S) u_3^n(y_S) \end{pmatrix} \frac{e^{i\beta_n |x_3 - y_3|}}{2}.$$

More generally, in the following $G_a^b$ will denote the tensor obtained from $G$ by selecting among the rows of matrix $G$ those who correspond to the components of type $a$ and by selecting among the columns of $G$ those who correspond to the components of type $b$, with

$a, b = u, \sigma, X, Y$.
With such notations, we emphasize the following symmetry relationships

$$G_u^\sigma(x,y) = {}^T G_u^\sigma(y,x), \quad G_u^Y(x,y) = -{}^T G_X^\sigma(y,x), \tag{16}$$

which are readily shown from the extended Green function given by (14) by using the notations (7). In the following, we discuss the Neumann crack problem, because it is the most interesting case from the point of view of applications, as mentioned in the introduction. We will give a few indications on the Dirichlet crack problem afterwards. We introduce some similar integral operators as those used in the acoustic case [8]. In this view, we define the differential operators $d_\nu$, $d_\nu^y$ and $\tilde{d}_\nu^x$ as follows. Denoting $d_\nu \mathbf{u} := \sigma(\mathbf{u})\cdot\boldsymbol{\nu}$ for some displacement vector $\mathbf{u}$, then for some $3\times 3$ tensor $M$ which is a function of $x$ and $y$, $d_\nu^y(M)$ is the $3\times 3$ tensor the rows of which are formed by the vectors $d_\nu(\mathbf{M}_i)$ with respect to variable $y$, where $\mathbf{M}_i$ is the $i$-th row of $M$, while $\tilde{d}_\nu^x(M)$ is the $3\times 3$ tensor the columns of which are formed by the vectors $d_\nu(\mathbf{M}_j)$ with respect to variable $x$, where $\mathbf{M}_j$ is the $j$-th column of $M$.
We now define the operator $T : \mathbf{H}^{\frac{1}{2}}(\partial D) \to \mathbf{H}^{-\frac{1}{2}}(\partial D)$ by

$$(T\boldsymbol{\phi})(x) := d_\nu \left( \int_{\partial D} d_\nu^y (G_u^\sigma(x,y)) \cdot \boldsymbol{\phi}(y)\, ds(y) \right), \quad x \in \partial D.$$

and its restriction to $\gamma$, namely $T_\gamma : \tilde{\mathbf{H}}^{\frac{1}{2}}(\gamma) \to \mathbf{H}^{-\frac{1}{2}}(\gamma)$, by

$$(T_\gamma\boldsymbol{\phi})(x) := d_\nu \left( \int_{\gamma} d_\nu^y (G_u^\sigma(x,y)) \cdot \boldsymbol{\phi}(y)\, ds(y) \right), \quad x \in \gamma.$$

The above operators have to be understood from a variational point of view in general, and for smooth $\boldsymbol{\phi}$ they are defined as Cauchy principal values. In this sense the operators $T$ and $T_\gamma$ are hypersingular. That $T$ maps $\mathbf{H}^{\frac{1}{2}}(\partial D)$ to $\mathbf{H}^{-\frac{1}{2}}(\partial D)$ is obtained by comparison with the equivalent operator $T_\infty$ obtained by replacing the Green function $G_u^\sigma$ by $\Phi$, where $\Phi$ is the radiating Green's tensor of elastodynamics in free space $\mathbb{R}^3$, the expression of which is

$$\Phi(x,y) = \frac{1}{\mu}\left( g_{k_s}(x,y)\mathrm{Id} + \frac{1}{k_s^2}\nabla_x^2 (g_{k_s} - g_{k_p}) \right), \tag{17}$$

where

$$g_\kappa(x,y) = \frac{e^{i\kappa|x-y|}}{4\pi|x-y|}, \quad k_S = \omega\sqrt{\frac{\rho}{\mu}}, \quad k_P = \omega\sqrt{\frac{\rho}{\lambda+2\mu}},$$

and $\nabla^2$ denotes the Hessian matrix. In particular, the singularity of $\Phi$ is like $1/|x-y|$. The mapping properties of $T_\infty$ are obtained in [4] (see also [1]), where the singularity of $T_\infty$ is treated from a variational point of view. Note that even if [4] is limited to $d = 2$, the analysis of $T_\infty$ contained therein is also valid for $d = 3$. For all $y \in W$, by subtracting the equations satisfied by $G_u^\sigma(\cdot, y)$ and $\Phi(\cdot, y)$ and by using regularity results for elliptic systems, we have $G_u^\sigma(\cdot, y) - \Phi(\cdot, y) \in (C^\infty(\overline{W}))^{3\times 3}$, so that the mapping properties of $T$ are the same as those of $T_\infty$. The proof of that result follows the lines of [20] (see paragraph 3 for the Helmholtz equation). It consists in deriving integral representation formulas by introducing a small ball

$B(y,\varepsilon)$ centered at a point $y \in \partial D$. The jump relationships are then obtained by passing to the limit $\varepsilon \to 0$, capturing the singularity at point $y$. This last step uses both the regularity of kernel $G_u^\sigma - \Phi$ and the jump relationships obtained in [4] (see also [17]) for kernel $\Phi$. In particular, if we consider the double layer potential

$$(\mathcal{D}\boldsymbol{\phi})(x) := \int_{\partial D} d_\nu^y(G_u^\sigma(x,y)) \cdot \boldsymbol{\phi}(y)\, ds(y), \quad x \in W \setminus \partial D$$

and its analogue $\mathcal{D}_\infty$ with the kernel $G_u^\sigma$ replaced by $\Phi$, we obtain that the displacement $((\mathcal{D}-\mathcal{D}_\infty)\boldsymbol{\phi})$ and its corresponding normal stress are continuous across $\partial D$. We then conclude that

$$\boldsymbol{\phi} = (\mathcal{D}_\infty\boldsymbol{\phi})_+ - (\mathcal{D}_\infty\boldsymbol{\phi})_- = (\mathcal{D}\boldsymbol{\phi})_+ - (\mathcal{D}\boldsymbol{\phi})_-,$$

$$T\boldsymbol{\phi} = d_\nu(\mathcal{D}\boldsymbol{\phi})_+ = d_\nu(\mathcal{D}\boldsymbol{\phi})_-.$$

As a corollary, the operators $T-T_\infty : \mathbf{H}^{\frac{1}{2}}(\partial D) \to \mathbf{H}^{-\frac{1}{2}}(\partial D)$ and $T_\gamma - T_{\gamma,\infty} : \tilde{\mathbf{H}}^{\frac{1}{2}}(\gamma) \to \mathbf{H}^{-\frac{1}{2}}(\gamma)$ are compact.

Let us also define the operator $G_N : \boldsymbol{g} \in \mathbf{H}^{-\frac{1}{2}}(\gamma) \to \mathbf{L}^2(\hat{S})$ which maps $\boldsymbol{g} \in \mathbf{H}^{-\frac{1}{2}}(\gamma)$ into the trace on $\hat{S}$ of the $\mathbf{X}$ extension of the solution to the Neumann crack problem (11) with data $\boldsymbol{g}$, as well as the integral operators $\mathcal{F}_N : \tilde{\mathbf{H}}^{\frac{1}{2}}(\gamma) \to \mathbf{L}^2(\hat{S})$ and $\mathcal{H}_N : \mathbf{L}^2(\hat{S}) \to \mathbf{H}^{-\frac{1}{2}}(\gamma)$ such that

$$(\mathcal{F}_N\boldsymbol{\phi})(x) := \int_\gamma d_\nu^y(G_X^\sigma(x,y)) \cdot \boldsymbol{\phi}(y)\, ds(y), \quad x \in \hat{S},$$

$$(\mathcal{H}_N\mathbf{h})(x) := \int_{\hat{S}} \tilde{d}_\nu^x(G_u^Y(x,y)) \cdot \mathbf{h}(y)\, ds(y), \quad x \in \gamma.$$

Let us give the following unique continuation lemma:

**Lemma 3.1.** *For all $s > R$, if the displacement field $\mathbf{u}$ satisfies*

$$\begin{cases} \mathrm{div}\sigma(\mathbf{u}) + \rho\omega^2\mathbf{u} = 0 & \text{in} \quad S \times (R,s) \\ \sigma(\mathbf{u}) \cdot \boldsymbol{\nu} = 0 & \text{on} \quad \Gamma \times (R,s) \\ \mathbf{X} = 0 & \text{on} \quad S_R \\ T_+\mathbf{Y} = \mathbf{X} & \text{on} \quad S_s, \end{cases}$$

*where $\mathbf{X}$ and $\mathbf{Y}$ are the extensions of $\mathbf{u}$, then $\mathbf{X}$, $\mathbf{Y}$ and $\mathbf{u}$ vanish in $S \times (R,s)$.*

*Proof.* The extension $(\mathbf{X},\mathbf{Y})$ of $\mathbf{u}$ satisfies the evolution problem (2) (3), the solutions of which are given by (4) (5). The radiation condition on $S_s$ implies that $a_n^- = 0$ for all $n > 0$ in (4). Let us prove this fact. We have on the transverse section $S_s$

$$\begin{pmatrix} \mathbf{X}_n^+ \\ \mathbf{Y}_n^+ \end{pmatrix} = \begin{pmatrix} \boldsymbol{\mathcal{X}}_n \\ \boldsymbol{\mathcal{Y}}_n \end{pmatrix} e^{i\beta_n s}, \quad \begin{pmatrix} \mathbf{X}_n^- \\ \mathbf{Y}_n^- \end{pmatrix} = \begin{pmatrix} -\boldsymbol{\mathcal{X}}_n \\ \boldsymbol{\mathcal{Y}}_n \end{pmatrix} e^{-i\beta_n s},$$

so that

$$T_+\mathbf{Y}_n^+ = \sum_{m>0} e^{i\beta_n s}(\boldsymbol{\mathcal{X}}_m, \boldsymbol{\mathcal{Y}}_n)\boldsymbol{\mathcal{X}}_m = e^{i\beta_n s}\boldsymbol{\mathcal{X}}_n = \mathbf{X}_n^+,$$

$$T_+\mathbf{Y}_n^- = \sum_{m>0} e^{-i\beta_n s}(\boldsymbol{\mathcal{X}}_m, \boldsymbol{\mathcal{Y}}_n)\boldsymbol{\mathcal{X}}_m = e^{-i\beta_n s}\boldsymbol{\mathcal{X}}_n = -\mathbf{X}_n^-.$$

By using the radiation condition on $S_s$,

$$T_+\mathbf{Y} - \mathbf{X} = 0 = \sum_{n>0} \left(a_n^+(T_+\mathbf{Y}_n^+ - \mathbf{X}_n^+) + a_n^-(T_+\mathbf{Y}_n^- - \mathbf{X}_n^-)\right) = 2\sum_{n>0} a_n^- e^{-i\beta_n s}\boldsymbol{\mathcal{X}}_n,$$

which implies the announced result.
Lastly, that $\mathbf{X} = 0$ on $S_R$ implies that $a_n^+ = 0$ for all $n > 0$ in (4). The result follows. □

Now we prove some properties of operators $T_\gamma$, $\mathcal{F}_N$, $\mathcal{H}_N$ and $G_N$.

**Lemma 3.2.** *The following assertions hold true under assumptions 2.2 and 2.6.*

*(i) The operator $T_\gamma$ is an isomorphism.*

*(ii) The operators $\mathcal{F}_N$ and $\mathcal{H}_N$ satisfy $\mathcal{F}_N = -\overline{\mathcal{H}_N^*}$.*

*(iii) The operators $\mathcal{F}_N$, $G_N$ and $T_\gamma$ satisfy $\mathcal{F}_N = G_N T_\gamma$.*

*(iv) The operator $G_N$ is compact, injective with dense range.*

*Proof.* The first assertion is proved by following the same lines as the proof of lemma 3.2 in [8]. However, for readers convenience we repeat the proof here. Let us denote $T_\infty$ and $T_{\gamma,\infty}$ the analogues of operators $T$ and $T_\gamma$ with the kernel $G_u^\sigma$ replaced by $\Phi$ given by (17). Similarly, the analogues of operators $T_\infty$ and $T_{\gamma,\infty}$ in the particular case $\omega = i$ are denoted by $T_{\infty,i}$ and $T_{\gamma,\infty,i}$. Take some $\boldsymbol{\phi} \in \tilde{\mathbf{H}}^{\frac{1}{2}}(\gamma)$ and consider $\tilde{\boldsymbol{\phi}}$ its extension by 0 in $\mathbf{H}^{\frac{1}{2}}(\partial D)$. Then we have

$$\langle -T_{\gamma,\infty,i}\boldsymbol{\phi}, \boldsymbol{\phi}\rangle_{\mathbf{H}^{-\frac{1}{2}}(\gamma),\tilde{\mathbf{H}}^{\frac{1}{2}}(\gamma)} = \left\langle -T_{\infty,i}\tilde{\boldsymbol{\phi}}, \tilde{\boldsymbol{\phi}}\right\rangle_{\mathbf{H}^{-\frac{1}{2}}(\partial D),\mathbf{H}^{\frac{1}{2}}(\partial D)}.$$

By theorem 3.3 in [4], $-T_{\infty,i}$ is a selfadjoint and coercive operator, so we have for some constant $c > 0$

$$\langle -T_{\gamma,\infty,i}\boldsymbol{\phi}, \boldsymbol{\phi}\rangle_{\mathbf{H}^{-\frac{1}{2}}(\gamma),\tilde{\mathbf{H}}^{\frac{1}{2}}(\gamma)} \geq c\,||\tilde{\boldsymbol{\phi}}||^2_{\mathbf{H}^{\frac{1}{2}}(\partial D)} = c\,||\boldsymbol{\phi}||^2_{\tilde{\mathbf{H}}^{\frac{1}{2}}(\gamma)},$$

which implies that $T_{\gamma,\infty,i}$ is an isomorphism. The operator $(T_\gamma - T_{\gamma,\infty,i}) = (T_\gamma - T_{\gamma,\infty}) + (T_{\gamma,\infty} - T_{\gamma,\infty,i})$ is compact as the sum of two compact operators. Indeed, we have already seen that the first one is compact, while the kernel of the second one is smooth, such kernel being the discrepancy between the tensor $\Phi$ given by (17) for some $\omega$ and the same tensor for $\omega = i$. With the help of the decomposition $T_\gamma = T_{\gamma,\infty,i} + (T_\gamma - T_{\gamma,\infty,i})$, it remains to prove that $T_\gamma$ is injective.

In this view, assume that for $\boldsymbol{\phi} \in \tilde{\mathbf{H}}^{\frac{1}{2}}(\gamma)$ we have $T_\gamma \boldsymbol{\phi} = T\tilde{\boldsymbol{\phi}} = 0$. Let us consider again the double layer potential

$$(\mathcal{D}\tilde{\boldsymbol{\phi}})(x) := \int_{\partial D} d_\nu^y(G_u^\sigma(x,y)) \cdot \tilde{\boldsymbol{\phi}}(y)\, ds(y), \quad x \in W \setminus \partial D.$$

We have already seen that

$$\tilde{\boldsymbol{\phi}} = (\mathcal{D}\tilde{\boldsymbol{\phi}})_+ - (\mathcal{D}\tilde{\boldsymbol{\phi}})_-,$$

$$T\tilde{\boldsymbol{\phi}} = d_\nu(\mathcal{D}\tilde{\boldsymbol{\phi}})_+ = d_\nu(\mathcal{D}\tilde{\boldsymbol{\phi}})_-.$$

Since $T\tilde{\boldsymbol{\phi}} = 0$, the function $(\mathcal{D}\tilde{\boldsymbol{\phi}})$ solves the Neumann crack problem (11) with $\boldsymbol{g} = 0$. The conjectured uniqueness for this problem implies that $(\mathcal{D}\tilde{\boldsymbol{\phi}})$ vanishes in $W \setminus \overline{\gamma}$, then $\tilde{\boldsymbol{\phi}}$ vanishes on $\partial D$, that is $\boldsymbol{\phi} = 0$ on $\gamma$. We have proved that $T_\gamma$ is injective.
Let us prove the second assertion. We have

$$(\mathcal{F}_N \boldsymbol{\phi}, \mathbf{h})_{\mathbf{L}^2(\hat{S})} = \int_{\hat{S}} \left( \int_\gamma d_\nu^x(G_X^\sigma(y,x)) \cdot \boldsymbol{\phi}(x)\, ds(x) \right) \cdot \overline{\mathbf{h}(y)}\, ds(y)$$

$$= \int_\gamma \boldsymbol{\phi}(x) \cdot \left( \int_{\hat{S}} {}^T[d_\nu^x(G_X^\sigma(y,x))] \cdot \overline{\mathbf{h}(y)}\, ds(y) \right) ds(x)$$

$$= \int_\gamma \boldsymbol{\phi}(x) \cdot \left( \int_{\hat{S}} \tilde{d}_\nu^x \left( {}^T[G_X^\sigma(y,x)] \right) \cdot \overline{\mathbf{h}(y)}\, ds(y) \right) ds(x)$$

so that by using the second symmetry relationship of (16),

$$(\mathcal{F}_N \boldsymbol{\phi}, \mathbf{h})_{\mathbf{L}^2(\hat{S})} = -\int_\gamma \boldsymbol{\phi}(x) \cdot \left( \int_{\hat{S}} \tilde{d}_\nu^x(G_u^Y(x,y)) \cdot \overline{\mathbf{h}(y)}\, ds(y) \right) ds(x)$$

$$= -\int_\gamma \boldsymbol{\phi}(x) \cdot (\mathcal{H}_N \overline{\mathbf{h}})(x)\, ds(x) = -\int_\gamma \boldsymbol{\phi}(x) \cdot \overline{(\mathcal{H}_N \mathbf{h})(x)}\, ds(x),$$

which completes the proof of the second assertion.
The third assertion is obvious.
Let us prove the last one. Compactness of $G_N$ is proved with the same argument as in lemma 3.2 of [8]. Assume that $G_N \boldsymbol{g} = 0$ for some $\boldsymbol{g} \in \mathbf{H}^{-\frac{1}{2}}(\gamma)$ and let us denote by $\mathbf{u}$ the solution of the Neumann crack problem (11) which is associated with data $\boldsymbol{g}$. Consider the extension $\mathbf{X}$ of $\mathbf{u}$. The trace of $\mathbf{X}$ vanishes on $S_R$, which from lemma 3.1 and unique continuation implies that $\mathbf{u} = 0$ in $W \setminus \overline{\gamma}$, so that $\boldsymbol{g} = 0$. This proves the injectivity of $G_N$. Now let us prove the injectivity of $\mathcal{H}_N$, which will imply that $G_N$ has dense range from the three previous assertions. Assume that $\mathcal{H}_N \mathbf{h} = 0$ for some $\mathbf{h} \in \mathbf{L}^2(\hat{S})$, which means that the function

$$(\mathbf{v_h})(x) := \int_{\hat{S}} G_u^Y(x,y) \cdot \mathbf{h}(y)\, ds(y), \quad x \in W \setminus \gamma$$

solves the Neumann crack problem (11) with $\boldsymbol{g} = 0$. Then $\mathbf{v_h}$ vanishes in $W_R \setminus \overline{\gamma}$, as well as its $\mathbf{X}$ extension denoted by $\mathbf{X_h}$. With the decomposition $\mathbf{h} = (\mathbf{h}_-, \mathbf{h}_+) \in \mathbf{L}^2(S_{-R}) \times \mathbf{L}^2(S_R)$, we have for $x_3 \in (-R, R)$,

$$(\mathbf{X_h})(x) = \int_{S_{-R}} G_X^Y(x,y) \cdot \mathbf{h}_-(y)\, ds(y) + \int_{S_R} G_X^Y(x,y) \cdot \mathbf{h}_+(y)\, ds(y).$$

From the expression of $G$ given by (14), we obtain

$$G_X^Y(x,y) = -\sum_{n>0} \frac{e^{i\beta_n|x_3-y_3|}}{2} \boldsymbol{\mathcal{X}}_n(x_S) \cdot {}^T\boldsymbol{\mathcal{X}}_n(y_S),$$

which together with the decompositions $\mathbf{h}_- = \sum_{n>0} h_n^- \boldsymbol{\mathcal{Y}}_n$ and $\mathbf{h}_+ = \sum_{n>0} h_n^+ \boldsymbol{\mathcal{Y}}_n$, implies

$$(\mathbf{X_h})(x) = -\sum_{n>0} \frac{h_n^-}{2} e^{i\beta_n(R+x_3)} \boldsymbol{\mathcal{X}}_n(x_S) - \sum_{n>0} \frac{h_n^+}{2} e^{i\beta_n(R-x_3)} \boldsymbol{\mathcal{X}}_n(x_S).$$

Since $\mathbf{X_h} = 0$ in $W_R \setminus \overline{\gamma}$, we obtain that $h_n^- e^{i\beta_n x_3} + h_n^+ e^{-i\beta_n x_3} = 0$ for an open interval of $x_3$, which implies ($\beta_n \neq 0$) that $h_n^- = h_n^+ = 0$ for all $n > 0$, that is $\mathbf{h} = 0$. The proof is complete. □

*3.2. The Linear Sampling Method*

We now introduce the Linear Sampling Method for the Neumann crack problem. In this view, we define the near field operator $F_N : \mathbf{L}^2(\hat{S}) \to \mathbf{L}^2(\hat{S})$, such that

$$(F_N\mathbf{h})(x) := \int_{\hat{S}} X_Y^s(x,y) \cdot \mathbf{h}(y)\, ds(y), \quad x \in \hat{S}, \tag{18}$$

where $X_Y^s(\cdot, y)$ is the $\mathbf{X}$ extension of the scattered field $U_Y^s(\cdot, y)$ associated with the incident field $G_u^Y(\cdot, y)$ for $y \in \hat{S}$. In other words the $j$-th column of matrix $U_Y^s(., y)$ is the solution of the Neumann crack problem (11) with data $\boldsymbol{g}$ set to the $j$-th column of $-\tilde{d}_\nu^x(G_u^Y(., y))$.
We obtain the following factorization for the Neumann crack problem.

**Proposition 3.3.** *The near field $F_N$ given by (18) has the factorization forms*

$$F_N = G_N \overline{T_\gamma^*}\, \overline{G_N^*} = -\mathcal{F}_N T_\gamma^{-1} \mathcal{H}_N.$$

*Proof.* The proof follows from the fact that $F_N = -G_N\mathcal{H}_N$ and the first three assertions of lemma 3.2. □

We have the following proposition, which specifies the choice of the test function in the LSM. The proof is omitted since it is similar to that of proposition 3.4 in [8], the only difference is that lemma 3.1 is used instead of the equivalent lemma 3.1 in [8].

**Proposition 3.4.** *For some crack $L$, let us denote by $\mathcal{F}_N^L : \tilde{\mathbf{H}}^{\frac{1}{2}}(L) \to \mathbf{L}^2(\hat{S})$ the analogue of $\mathcal{F}_N$ when $\gamma$ is replaced by $L$. For some continuous vector function $\boldsymbol{\beta} \in \tilde{\mathbf{H}}^{\frac{1}{2}}(L)$ satisfying $|\boldsymbol{\beta}| > 0$ on $L$, for the Neumann crack problem we have*

$$L \subset \gamma \quad \textit{if and only if} \quad \mathcal{F}_N^L \boldsymbol{\beta} \in \mathrm{R}(G_N).$$

We complete this subsection by the main theorem that (partially) justifies the LSM for elasticity, the proof of which is also omitted since it is the same as that of theorem 3.6 of [8] for the acoustic case. It is based on lemma 3.2 and propositions 3.3 and 3.4.

**Theorem 3.5.** *Let $F_N : \mathbf{L}^2(\hat{S}) \to \mathbf{L}^2(\hat{S})$ be the near field operator defined by (18) where $X_Y^s(\cdot, y)$ is the $\mathbf{X}$ extension of the scattered field $U_Y^s(\cdot, y)$ solving the Neumann crack problem (11) with the incident field $G_u^Y(\cdot, y)$ for $y \in \hat{S}$.*

*Let us define, for some continuous function $\boldsymbol{\beta} \in \tilde{\mathbf{H}}^{\frac{1}{2}}(L)$ with $|\boldsymbol{\beta}| > 0$ on $L$, the test function*

$$(\mathcal{F}_N^L \boldsymbol{\beta})(x) := \int_L d_\nu^y(G_X^\sigma(x, y)) \cdot \boldsymbol{\beta}(y)\, ds(y), \quad x \in \hat{S},$$

*and for $\varepsilon > 0$ and $I$ the identity on $\mathbf{L}^2(\hat{S})$, the Tikhonov operator $T_\varepsilon(F_N)$ associated with $F_N$, that is*

$$T_\varepsilon(F_N) := (\varepsilon I + F_N^* F_N)^{-1} F_N^*.$$

*For $\mathbf{h}_\varepsilon := T_\varepsilon(F_N)(\mathcal{F}_N^L \boldsymbol{\beta})$, we have*

$$L \not\subset \gamma \quad \textit{implies that} \quad \lim_{\varepsilon \to 0} ||\mathbf{h}_\varepsilon||_{\mathbf{L}^2(\hat{S})} = +\infty.$$

Concerning the Dirichlet crack problem, we obtain a similar theorem as 3.5 by considering the near field operator $F_D$ associated with the $\mathbf{X}$ extension of the solution $U_Y^s(\cdot, y)$ to the Dirichlet crack problem (11) with data $\boldsymbol{f}$ set to the columns of tensor $-G_u^Y(\cdot, y)|_\gamma$. In this case the test function is defined by

$$(\mathcal{F}_D^L \boldsymbol{\alpha})(x) := \int_L G_X^\sigma(x, y) \cdot \boldsymbol{\alpha}(y)\, ds(y), \quad x \in \hat{S},$$

where $\boldsymbol{\alpha}$ is some continuous vector function in $\tilde{\mathbf{H}}^{-\frac{1}{2}}(\gamma)$ with $|\boldsymbol{\alpha}| > 0$ on $L$.

Note that in such case the isomorphism $T_\gamma$ of proposition 3.3 is replaced by $S_\gamma : \tilde{\mathbf{H}}^{-\frac{1}{2}}(\gamma) \to \mathbf{H}^{\frac{1}{2}}(\gamma)$ defined by

$$(S_\gamma \boldsymbol{\phi})(x) := \int_\gamma G_u^\sigma(x, y) \cdot \boldsymbol{\phi}(y)\, ds(y), \quad x \in \gamma.$$

As in the acoustic case [8], we consider some infinitesimal cracks $L$ at point $z \in W$ and oriented by normal $\boldsymbol{\nu}(z)$. We specify $\boldsymbol{\alpha}$ and $\boldsymbol{\beta}$ as

$$\boldsymbol{\alpha} = \alpha_0\, \boldsymbol{p}, \quad \boldsymbol{\beta} = \beta_0\, \boldsymbol{e}_3,$$

where $\boldsymbol{p}$ is a vector such that $|\boldsymbol{p}| = 1$, and $\int_L \alpha_0\, ds = \int_L \beta_0\, ds = 1$, so that we make the approximations

$$\mathcal{F}_D^L \boldsymbol{\alpha} \simeq \mathbf{f}_D^z := G_X^\sigma(\cdot, z) \cdot \boldsymbol{p}, \quad \mathcal{F}_N^L \boldsymbol{\beta} \simeq \mathbf{f}_N^z := d_\nu^y(G_X^\sigma(\cdot, z)) \cdot \boldsymbol{e}_3. \tag{19}$$

*3.3. The modal formulation*

Now we come back to the inverse problem (IP). We have to express the kernel $X_Y^s(\cdot, y)$ of the near field operator (18) for $y \in \hat{S}$ only in terms of the $\mathbf{X}$ extension of the scattered fields $\mathbf{U}_n^{s\pm}$ associated with the incident fields $\mathbf{U}_n^{\pm}$ for $n > 0$, that is $\mathbf{X}_n^{s\pm}$.
In this view, we remark that

$$G_u^Y(x,y) = \begin{cases} \displaystyle\sum_{n>0} \frac{1}{2} \mathbf{U}_n^+(x) \cdot {}^T\mathbf{X}_n^-(y), & \text{for} \quad x_3 > y_3 \\ \displaystyle\sum_{n>0} \frac{1}{2} \mathbf{U}_n^-(x) \cdot {}^T\mathbf{X}_n^+(y), & \text{for} \quad x_3 < y_3, \end{cases}$$

which immediately implies that

$$X_Y^s(x,y) = \begin{cases} \displaystyle\sum_{n>0} \frac{1}{2} \mathbf{X}_n^{s^+}(x) \cdot {}^T\mathbf{X}_n^-(y), & \text{for} \quad x_3 > y_3 \\ \displaystyle\sum_{n>0} \frac{1}{2} \mathbf{X}_n^{s^-}(x) \cdot {}^T\mathbf{X}_n^+(y), & \text{for} \quad x_3 < y_3. \end{cases}$$

We denote $\mathbf{h} = (\mathbf{h}^-, \mathbf{h}^+) \in \mathbf{L}^2(S_{-R}) \times \mathbf{L}^2(S_R)$.
By using the modal decomposition of the unknowns

$$\mathbf{h}^- = -\sum_{n>0} h_n^- \boldsymbol{\mathcal{Y}}_n \qquad \text{and} \qquad \mathbf{h}^+ = \sum_{n>0} h_n^+ \boldsymbol{\mathcal{Y}}_n,$$

and the modal decomposition of the data

$$\begin{cases} \mathbf{X}_n^{s^+}(x) = \displaystyle\sum_{m>0} (A_n^+)_m^- \boldsymbol{\mathcal{X}}_m \text{ and } \mathbf{X}_n^{s^-} = \sum_{m>0} (A_n^-)_m^- \boldsymbol{\mathcal{X}}_m \quad \text{for} \quad x \in S_{-R} \\ \mathbf{X}_n^{s^+}(x) = \displaystyle\sum_{m>0} (A_n^+)_m^+ \boldsymbol{\mathcal{X}}_m \text{ and } \mathbf{X}_n^{s^-} = \sum_{m>0} (A_n^-)_m^+ \boldsymbol{\mathcal{X}}_m \quad \text{for} \quad x \in S_R, \end{cases}$$

the same computations as in [6] imply that for the Neumann crack problem the near field operator $F_N$ defined by (18) is also given by

$$\begin{cases} (F_N \mathbf{h})|_{S_{-R}} &= \displaystyle\sum_{m>0} \sum_{n>0} \frac{e^{i\beta_n R}}{2} \left( (A_n^+)_m^- h_n^- + (A_n^-)_m^- h_n^+ \right) \boldsymbol{\mathcal{X}}_m \\ (F_N \mathbf{h})|_{S_R} &= \displaystyle\sum_{m>0} \sum_{n>0} \frac{e^{i\beta_n R}}{2} \left( (A_n^+)_m^+ h_n^- + (A_n^-)_m^+ h_n^+ \right) \boldsymbol{\mathcal{X}}_m. \end{cases} \tag{20}$$

Note that for the Dirichlet crack problem the expression of the near field operator $F_D$ is the same as above, provided that the data $\mathbf{X}_n^{s^\pm}$ correspond to the Dirichlet crack problem instead of the Neumann crack problem. It remains to give a decomposition of the approximated test functions $\mathbf{f}_D^z$ and $\mathbf{f}_N^z$ given by (19) and used in theorem 3.5, $\mathbf{f}_D^z$ and $\mathbf{f}_N^z$ being associated with

the Dirichlet and the Neumann crack problem, respectively.
In this view we remark that

$$G_X^\sigma(x,y) = \begin{cases} -\sum_{m>0} \frac{1}{2} \mathbf{X}_m^+(x) \cdot {}^T\mathbf{U}_m^-(y), & \text{for} \quad x_3 > y_3 \\ -\sum_{m>0} \frac{1}{2} \mathbf{X}_m^-(x) \cdot {}^T\mathbf{U}_m^+(y), & \text{for} \quad x_3 < y_3. \end{cases} \tag{21}$$

Let us consider the Dirichlet case first. We have from (19),

$$\mathbf{f}_D^z(x) = \begin{cases} -\sum_{m>0} \frac{1}{2} \mathbf{X}_m^-(x)(\mathbf{U}_m^+(z) \cdot \boldsymbol{p}), & \text{for} \quad x \in S_{-R} \\ -\sum_{m>0} \frac{1}{2} \mathbf{X}_m^+(x)(\mathbf{U}_m^-(z) \cdot \boldsymbol{p}), & \text{for} \quad x \in S_R. \end{cases}$$

With decomposition $\boldsymbol{p} = (\boldsymbol{p}_S, p_3)$, we obtain

$$\begin{cases} \mathbf{f}_D^z|_{S_{-R}} &= \sum_{m>0} \frac{1}{2} (\boldsymbol{u}_S^m(z_S) \cdot \boldsymbol{p}_S + u_3^m(z_S) p_3) e^{i\beta_m(R+z_3)} \boldsymbol{\mathcal{X}}_m \\ \mathbf{f}_D^z|_{S_R} &= \sum_{m>0} \frac{1}{2} (-\boldsymbol{u}_S^m(z_S) \cdot \boldsymbol{p}_S + u_3^m(z_S) p_3) e^{i\beta_m(R-z_3)} \boldsymbol{\mathcal{X}}_m. \end{cases} \tag{22}$$

Concerning the Neumann case, we obtain from (21) that

$$d_\nu^y(G_X^\sigma(x,y)) = \begin{cases} -\sum_{m>0} \frac{1}{2} \mathbf{X}_m^+(x) \cdot {}^T\big(\sigma(\mathbf{U}_m^-(y)) \cdot \boldsymbol{\nu}(y)\big), & \text{for} \quad x_3 > y_3 \\ -\sum_{m>0} \frac{1}{2} \mathbf{X}_m^-(x) \cdot {}^T\big(\sigma(\mathbf{U}_m^+(y)) \cdot \boldsymbol{\nu}(y)\big), & \text{for} \quad x_3 < y_3, \end{cases}$$

and then from (19) that

$$\mathbf{f}_N^z(x) = \begin{cases} -\sum_{m>0} \frac{1}{2} \mathbf{X}_m^-(x) \left( {}^T\boldsymbol{\nu}(z) \cdot \sigma(\mathbf{U}_m^+(z)) \cdot \boldsymbol{e}_3 \right), & \text{for} \quad x \in S_{-R} \\ -\sum_{m>0} \frac{1}{2} \mathbf{X}_m^+(x) \left( {}^T\boldsymbol{\nu}(z) \cdot \sigma(\mathbf{U}_m^-(z)) \cdot \boldsymbol{e}_3 \right), & \text{for} \quad x \in S_R. \end{cases}$$

With decomposition $\boldsymbol{\nu} = (\boldsymbol{\nu}_S, \nu_3)$, we obtain

$$\begin{cases} \mathbf{f}_N^z|_{S_{-R}} &= \sum_{m>0} \frac{1}{2} (\boldsymbol{t}_S^m(z_S) \cdot \boldsymbol{\nu}_S(z) - t_3^m(z_S) \nu_3(z)) e^{i\beta_m(R+z_3)} \boldsymbol{\mathcal{X}}_m \\ \mathbf{f}_N^z|_{S_R} &= \sum_{m>0} \frac{1}{2} (\boldsymbol{t}_S^m(z_S) \cdot \boldsymbol{\nu}_S(z) + t_3^m(z_S) \nu_3(z)) e^{i\beta_m(R-z_3)} \boldsymbol{\mathcal{X}}_m. \end{cases} \tag{23}$$

As a conclusion, we are in a position to apply theorem 3.5 by using the modal decomposition of the near field operator given by (20) for data produced by the Neumann crack problem, and the equivalent theorem for data produced by the Dirichlet crack problem. We can see that the test function has to be properly chosen if the boundary condition on the crack is known *a priori*. In the Dirichlet case, the test function $\mathbf{f}_D^z$ given by the decomposition (22)

shall be used, while in the Neumann case the test function $\mathbf{f}_N^z$ given by the decomposition (23) shall be used. Note that the Linear Sampling Method amounts to solve, in the Tikhonov sense, the infinite system

$$\left\{\begin{array}{l} \displaystyle\sum_{n>0} e^{i\beta_n R}\left((A_n^+)_m^- h_n^- + (A_n^-)_m^- h_n^+\right) = e^{i\beta_m(R+z_3)}(\boldsymbol{u}_S^m(z_S)\cdot\boldsymbol{p}_S + u_3^m(z_S)p_3) \\ \displaystyle\sum_{n>0} e^{i\beta_n R}\left((A_n^+)_m^+ h_n^- + (A_n^-)_m^+ h_n^+\right) = e^{i\beta_m(R-z_3)}(-\boldsymbol{u}_S^m(z_S)\cdot\boldsymbol{p}_S + u_3^m(z_S)p_3) \end{array}\right. \quad \forall m>0$$

for the Dirichlet case and the infinite system

$$\left\{\begin{array}{l} \displaystyle\sum_{n>0} e^{i\beta_n R}\left((A_n^+)_m^- h_n^- + (A_n^-)_m^- h_n^+\right) = e^{i\beta_m(R+z_3)}(\boldsymbol{t}_S^m(z_S)\cdot\boldsymbol{\nu}_S(z) - t_3^m(z_S)\nu_3(z)) \\ \displaystyle\sum_{n>0} e^{i\beta_n R}\left((A_n^+)_m^+ h_n^- + (A_n^-)_m^+ h_n^+\right) = e^{i\beta_m(R-z_3)}(\boldsymbol{t}_S^m(z_S)\cdot\boldsymbol{\nu}_S(z) + t_3^m(z_S)\nu_3(z)) \end{array}\right. \quad \forall m>0$$

for the Neumann case.

By looking at the right-hand side of the first equation of each system, we can say that polarization is $\boldsymbol{u}_S\cdot\boldsymbol{p}_S + u_3p_3$ for any unit vector $\boldsymbol{p} = (\boldsymbol{p}_S, p_3)$ in the first case, while polarization is $\boldsymbol{t}_S\cdot\boldsymbol{\nu}_S - t_3\nu_3$ and hence is related to the unit normal $\boldsymbol{\nu}(z)$ to the crack in the second case. In practice, the unit normal to the crack $\boldsymbol{\nu}(z)$ is unknown and in the Neumann case it may be chosen by the same minimization process as in [8], which is recalled hereafter. This can also be applied to the Dirichlet case in order to optimize the unit vector $\boldsymbol{p}$.

The far field formulation of the Linear Sampling Method is obtained by restricting all the sums above to the $n_p$ propagating modes (see [7] for a discussion on the negative role of non-propagating modes).

### *3.4. Some numerical experiments*

In our numerical experiments, we consider a 2D waveguide of section $S = (-h, h)$. The obtained 2D model can be viewed as a 3D situation provided we assume that the medium is invariant with respect to direction $x_2$ and if we restrict to the Lamb modes. Actually, the invariance with respect to $x_2$ implies that we can separate solutions such that $u_1 = u_3 = 0$, which correspond to the $SH$ waves (shear waves with horizontal polarization), and the solutions such that $u_2 = 0$, which correspond to the so-called Lamb waves or $P-SV$ waves (coupling the pressure waves and the shear waves with polarization in the vertical plane). The first family of $SH$ waves amounts to a 2D acoustic problem, while the second family of Lamb modes corresponds to a $2D$ elasticity problem, which is the framework of our numerical study. For a comprehensive description of Lamb modes, the reader will refer to [23].

We now apply the modal far field formulation of the Linear Sampling Method, the number of propagating modes $n_p$ being given as a function of the frequency $\omega$. The synthetic data $\mathbf{X}_n^{s\pm}$ are obtained by using a finite element approximation of a weak formulation of problem (11). Such a weak formulation is detailed in [3].

*3.4.1. About noisy data* In practice, the data $\mathbf{X}_n^{s\pm}|_{S_{-R}}$ and $\mathbf{X}_n^{s\pm}|_{S_R}$ are contaminated by some noise of amplitude $\delta$, and the parameter $\varepsilon$ in the Tikhonov regularization is chosen as a function of $\delta$ following the Morozov's strategy introduced in [15] in the framework of the Linear Sampling Method. In our modal far field formulation, we exactly use the same Morozov's technique as in [7] to choose $\varepsilon$. The noisy data are obtained artificially by applying to each "exact" data some pointwise Gaussian noise which is then calibrated in order to obtain some noisy data such that the resulting relative amplitude of noise in $L^2$ norm be exactly some prescribed $\sigma$. More details concerning noisy data are given in [8].

*3.4.2. About polarization* Concerning the test function in the LSM, the polarization for the case of 2D Dirichlet crack problems is $u_1\,p_1 + u_3\,p_3$, where $(p_1, p_3)$ is any unit vector while the polarization for 2D Neumann crack problems is $t_1\,\nu_1 - t_3\,\nu_3 = \sigma_{31}\,\nu_1 + \sigma_{33}\,\nu_3$, where $(\nu_1, \nu_3)$ is the unit normal to the crack. As discussed in the introduction, the Dirichlet case is of limited interest from the point of view of applications, while the Neumann case corresponds to the usual defect we expect in an elastic (for instance metallic) material. For that reason, only Neumann cracks will be tested in our numerical experiments. The normal to the crack $(\nu_1, \nu_3)$ is unknown and determined by searching for each sampling point $z$ the angle $\theta$ such that $(\nu_1, \nu_3) = (\cos\theta, \sin\theta)$ minimizes $||\mathbf{h}_\varepsilon||_{\mathbf{L}^2(\hat{S})}$ in the spirit of theorem 3.5 and following the method introduced in [5] and reproduced in [8]. More precisely, for each $z$ we replace $\boldsymbol{\nu}(z) = (\nu_1(z), \nu_3(z))$ in the polarization $\sigma_{31}\,\nu_1(z) + \sigma_{33}\,\nu_3(z)$ by some arbitrary unit vector $(\cos\theta, \sin\theta)$. For $\theta = 0$ and $\theta = \pi/2$, we compute the corresponding functions $\mathbf{h}_{\varepsilon,1}$ and $\mathbf{h}_{\varepsilon,3}$. By linearity the function $\mathbf{h}_\varepsilon$ which corresponds to vector $(\cos\theta, \sin\theta)$ is

$$\mathbf{h}_\varepsilon = (\cos\theta)\,\mathbf{h}_{\varepsilon,1} + (\sin\theta)\,\mathbf{h}_{\varepsilon,3}, \tag{24}$$

and a straightforward computation enables us to obtain the angle $\theta$ that minimizes $||\mathbf{h}_\varepsilon||_{\mathbf{L}^2(\hat{S})}$. In the figures hereafter, we have plotted the optimal $\log(1/||\mathbf{h}_\varepsilon||_{\mathbf{L}^2(\hat{S})})$ for each $z$. Following theorem 3.5, the complementary part of the crack reads as the set of points $z$ for which the above function vanishes.

*3.4.3. Numerical results* The height of the waveguide is $2h$ with $h = 0.01\,m$. The sampling grid is limited by $S_{-R}$ and $S_R$ with $R = 0.01\,m$. The material is steel with density $\rho = 7800\,kg/m^3$, Lamé constants $\lambda = 1.1277\,10^{11}\,Pa$ and $\mu = 7.9374\,10^{10}\,Pa$. In order to emphasize the impact of the polarization on the efficiency of the LSM we consider a curved crack. As already observed in [7, 8, 6] in acoustics or elasticity, the bigger is the number of propagating modes $n_p$ (or equivalently the larger is the frequency $\omega$) the better is the identification. This is the reason why we do not show the effect of $n_p$ in the present paper and consider only the case $n_p = 20$ (which corresponds to $\omega = 10^6\,Hz$), for which the smaller wavelength associated with the propagating modes has approximately the size of the defect. First the amplitude of relative noise is $\sigma = 0.01$. The results of identification are given on

figure 2 for different global choices of polarization (that is such choice is independent of $z$), namely $u_1$, $u_3$, $t_1$ and $t_3$, as well as the result obtained by our local optimization procedure to obtain the normal to the crack. We remark that the result is very poor with an imposed displacement polarization, is better for an imposed stress polarization, in particular in the area of the crack where the polarization coincides with the true orientation of the crack, and is very good when the polarization is optimized at each sampling point. In figures 3 and 4 we study the influence of the amplitude of noise, for $n_p = 20$. We consider a set of two curved Neumann cracks, for the suitable Neumann test function and with optimized polarization. The results correspond to $\sigma = 0.01$, $\sigma = 0.05$ and $\sigma = 0.1$. Figure 3 refers to some cracks that are far away from each other, while figure 4 refers to some cracks that are close to each other, which is a tricky case.


## Acknowledgements

The authors are indebted to Alexandre Routier for his work on their codes during his training in the laboratory POEMS.


## References


[1] M. S. Agranovich, B. A. Amosov, and M. Levitin, *Spectral problems for the Lamé system with spectral parameter in boundary conditions on smooth or nonsmooth boundary*, Russ. J. Math. Phys., 6 (1999), pp. 247–281.

[2] K. Baganas, B. B. Guzina, A. Charalambopoulos, and G. D. Manolis, *A linear sampling method for the inverse transmission problem in near-field elastodynamics*, Inverse Problems, 22 (2006), pp. 1835–1853.

[3] V. Baronian, A.-S. Bonnet-BenDhia, and E. Lunéville, *Transparent boundary conditions for the harmonic diffraction problem in an elastic waveguide*, J. Comput. Appl. Math, (2009), pp. 1945–1952.

[4] E. Bécache and T. H. Duong, *A space-time variational formulation for the boundary integral equation in a 2d elastic crack problem*, RAIRO M2AN, 28 (1994).

[5] F. Ben Hassen, Y. Boukari, and H. Haddar, *Application of the linear sampling method to retrieve cracks with impedance boundary conditions*, Rapport de recherche RR-7478, INRIA, Dec. 2010.

[6] L. Bourgeois, F. Le Louer, and E. Lunéville, *On the use of lamb modes in the linear sampling method for elastic waveguides*, Inverse Problems, 27 (2011), p. 055001.

[7] L. Bourgeois and E. Lunéville, *The linear sampling method in a waveguide: a modal formulation*, Inverse Problems, 24 (2008), p. 015018.

[8] ——, *On the use of sampling methods to identify cracks in acoustic waveguides*, Inverse Problems, 28 (2012), p. 105011.

[9] F. Cakoni and D. Colton, *Qualitative methods in inverse scattering theory*, Interaction of Mechanics and Mathematics, Springer-Verlag, Berlin, 2006. An introduction.

[10] A. Charalambopoulos, D. Gintides, and K. Kiriaki, *The linear sampling method for the transmission problem in three-dimensional linear elasticity*, Inverse Problems, 18 (2002), pp. 547–558.

[11] ——, *The linear sampling method for non-absorbing penetrable elastic bodies*, Inverse Problems, 19 (2003), pp. 549–561.

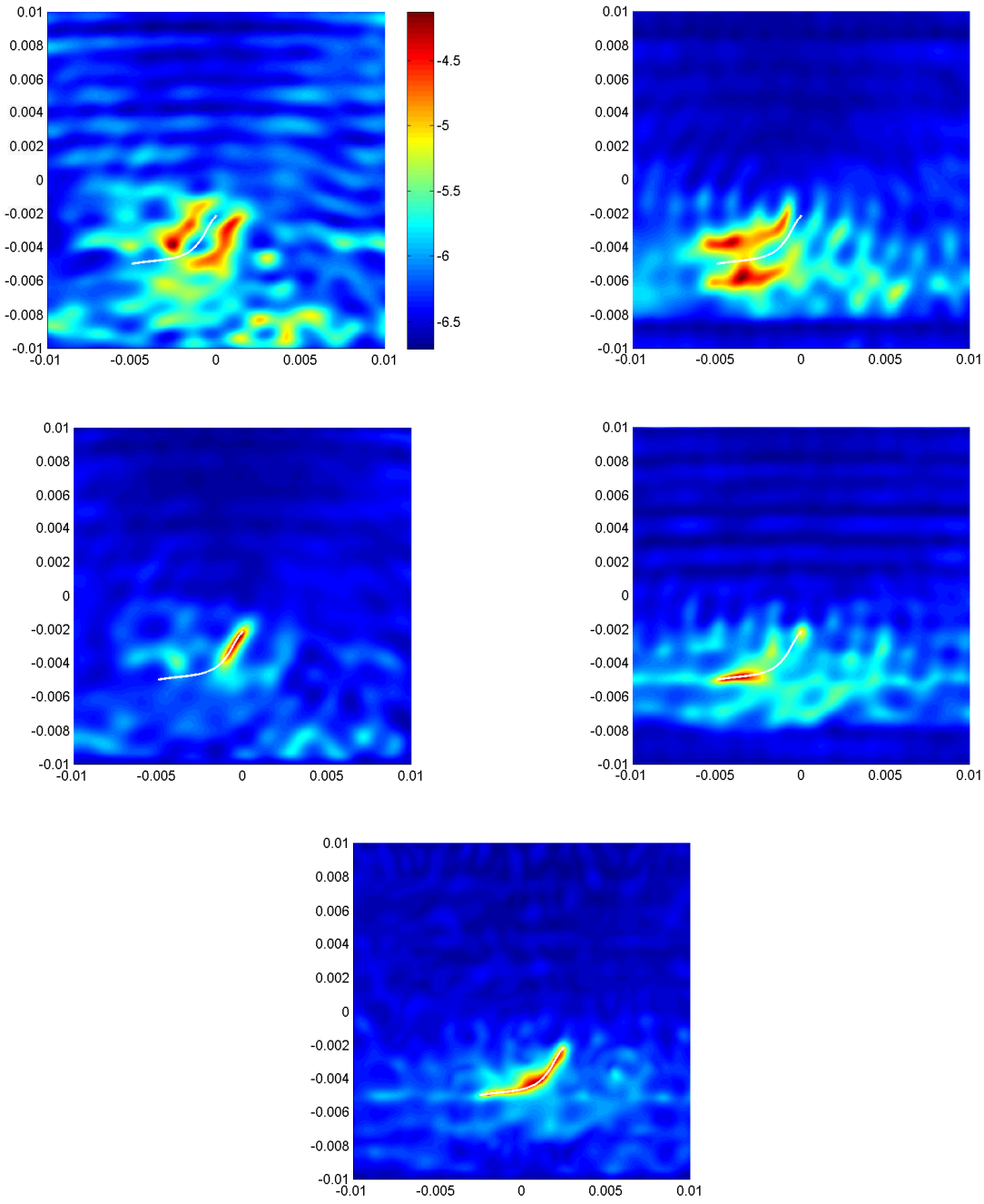


**Figure 2.** Top left: polarization $u_1$, Top right: polarization $u_3$, Middle left: polarization $t_1$, Middle right: polarization $t_3$, Bottom: optimized polarization. The real crack is represented in blank.

[12] A. Charalambopoulos, D. Gintides, K. Kiriaki, and A. Kirsch, *The factorization method for an acoustic wave guide*, 7th Int. Workshop on Mathematical Methods in Scattering Theory and

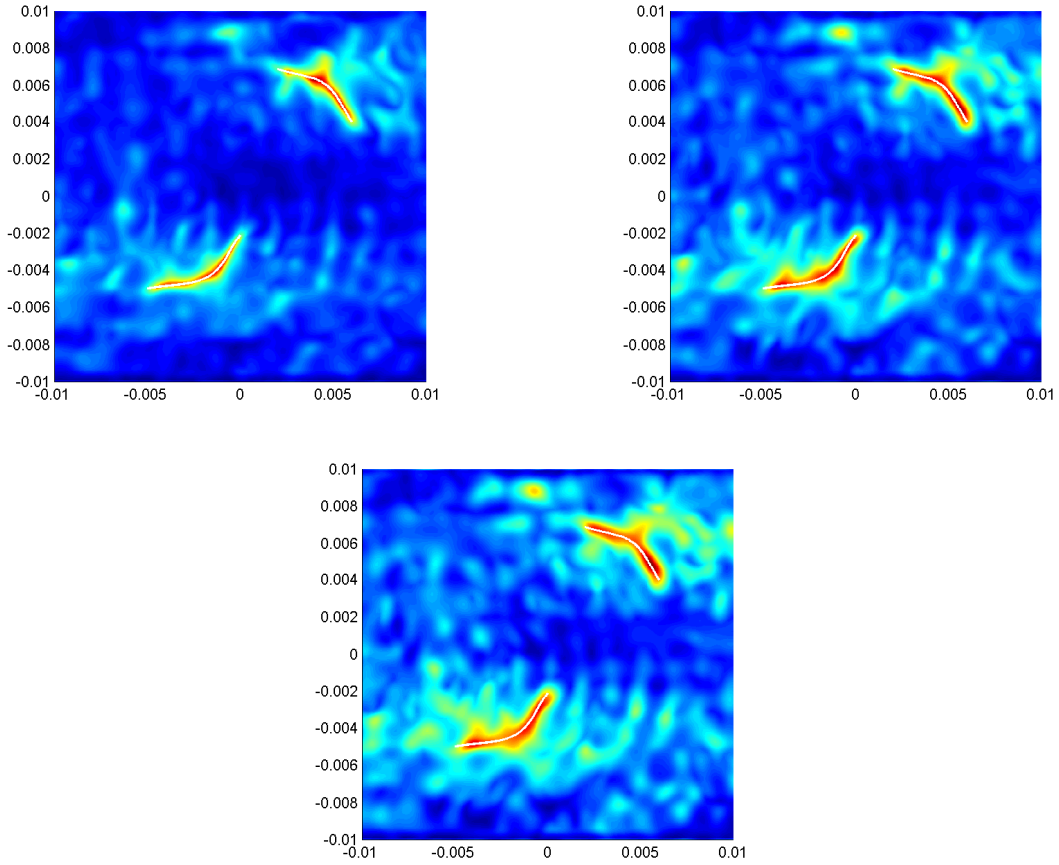


**Figure 3.** Top left: $\sigma = 0.01$, Top right: $\sigma = 0.05$, Bottom: $\sigma = 0.1$

Biomedical Engineering, (2006), pp. 120–127.

[13] A. Charalambopoulos, A. Kirsch, K. A. Anagnostopoulos, D. Gintides, and K. Kiriaki, *The factorization method in inverse elastic scattering from penetrable bodies*, Inverse Problems, 23 (2007), pp. 27–51.

[14] D. Colton and A. Kirsch, *A simple method for solving inverse scattering problems in the resonance region*, Inverse Problems, 12 (1996), pp. 383–393.

[15] D. Colton, M. Piana, and R. Potthast, *A simple method using morozov's discrepancy principle for solving inverse scattering problems*, Inverse Problems, 13 (1997), pp. 1477–1493.

[16] W. B. Fraser, *Orthogonality relation for the rayleigh-lamb modes of vibration of a plate*, J. Acoust. Soc. Am., 59 (1976), pp. 215–216.

[17] T. Ha-Duong, *On the boundary integral equations for the crack opening displacement of flat cracks*, Integral Equations Operator Theory, 15 (1992), pp. 427–453.

[18] A. Kirsch and N. Grinberg, *The factorization method for inverse problems*, vol. 36 of Oxford Lecture Series in Mathematics and its Applications, Oxford University Press, Oxford, 2008.

[19] A. Kirsch and S. Ritter, *A linear sampling method for inverse scattering from an open arc*, Inverse Problems, 16 (2000), pp. 89–105.

[20] J.-C. Nédélec, *Acoustic and Electromagnetic Equations*, Springer-Verlag, 2001.

[21] S. Nintcheu Fata and B. B. Guzina, *A linear sampling method for near-field inverse problems in*

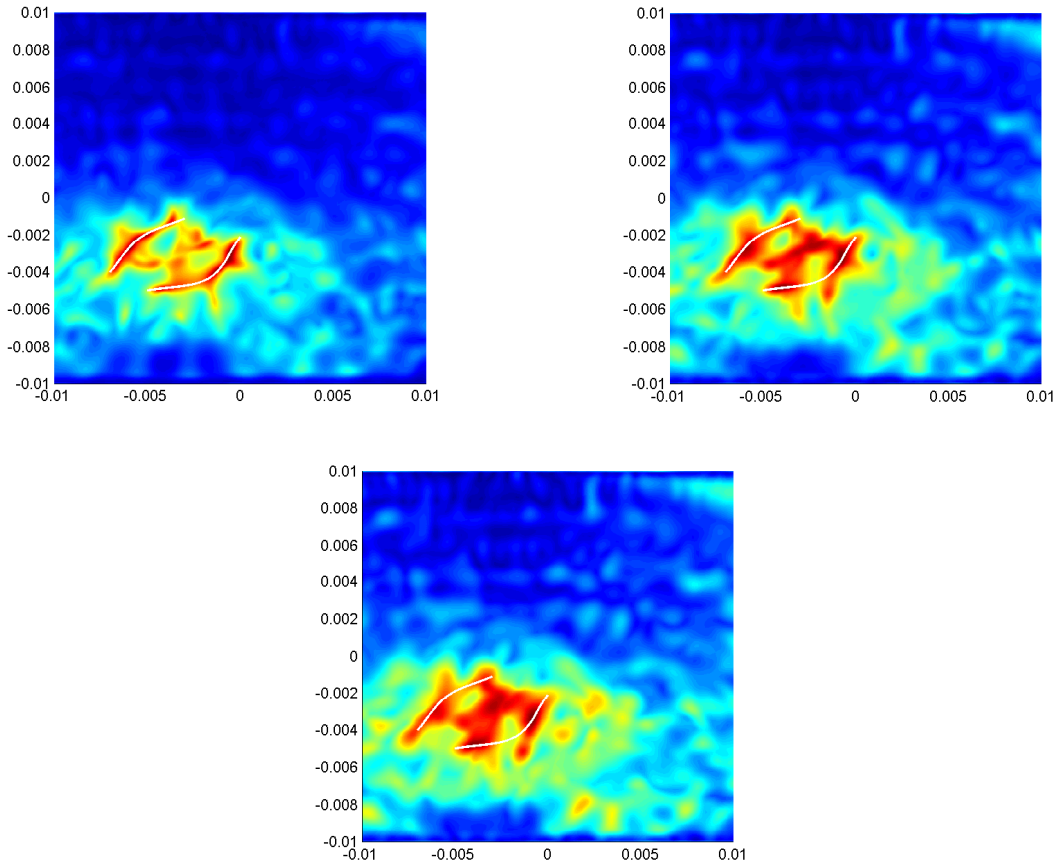


**Figure 4.** Top left: $\sigma = 0.01$, Top right: $\sigma = 0.05$, Bottom: $\sigma = 0.1$

*elastodynamics*, Inverse Problems, 20 (2004), pp. 713–736.

[22] V. Pagneux and A. Maurel, *Lamb wave propagation in elastic waveguides with variable thickness*, Proc. R. Soc. Lond. Ser. A Math. Phys. Eng. Sci., 462 (2006), pp. 1315–1339.

[23] F. Royer Daniel and E. Dieulesaint, *Ondes élastiques dans les solides*, Interaction of Mechanics and Mathematics, Masson, Paris, 1996. Tomes 1, Propagation libre et guidée.

[24] Y. Xu, C. Mawata, and W. Lin, *Generalized dual space indicator method for underwater imaging*, Inverse Problems, 16 (2000), pp. 1761–1776.